

Use of Archived Data and Geospatial Methods for Characterising Sundarbans

Sanjeev Kumar Srivastava , Prashant K. Srivastava, Harikesh Singh, Sharif A. Mukul, Mohammed A. S. Arfin-Khan, Mukunda Dev Behera, and Dhananjay Barman

Abstract The Sundarbans, designated as a UNESCO World Heritage Site and recognised as the world’s largest contiguous mangrove forest, is an ecologically critical region. This unique ecosystem faces significant vulnerability to a range of natural hazards, including cyclones, coastal erosion, land loss, and pollution—all of which contribute to the degradation of its biodiversity and the disruption of essential ecosystem services. Addressing these multifaceted challenges demands an integrated, transboundary approach that harmonises ecological conservation with socioeconomic development. This involves not only safeguarding forest habitats but also enhancing livelihoods and reducing poverty among local communities. To enable a comprehensive analysis of both the Indian and Bangladesh parts of the Sundarbans, it is vital to leverage temporal insights from archived geospatial data sets—such as historical topographic maps, declassified satellite-based photographs, and satellite imagery from various Earth observation platforms. In this chapter, we examine a

S. K. Srivastava (✉) · H. Singh
School of Science Technology and Engineering (SSTE), University of the Sunshine Coast,
Sippy Downs, QLD, Australia
e-mail: sanjeev.srivastava@usc.edu.au; ssrivast@usc.edu.au

P. K. Srivastava
Remote Sensing Laboratory, Institute of Environment and Sustainable Development, Banaras
Hindu University, Varanasi, India

S. A. Mukul
Department of Environment and Development Studies, United International University,
Dhaka, Bangladesh

M. A. S. Arfin-Khan
Department of Forestry and Environmental Science, Shahjalal University of Science and
Technology, Sylhet, Bangladesh

M. D. Behera
Centre for Ocean, River, Atmosphere and Land Sciences (CORAL), Indian Institute of
Technology Kharagpur, Kharagpur, India

D. Barman
ICAR—Central Research Institute for Jute and Allied Fibers, Kolkata, India

19 variety of data sources that can offer more in-depth insights into the dynamics of
20 this ecosystem. We also compare the utility of contemporary remote sensing data
21 with archived information dating back to the mid-eighteenth century.

22 **Keywords** Archived data · Geospatial data · Remote sensing · Mangrove forest ·
23 Sundarbans

24 1 Introduction

25 The Sundarbans, the world's largest contiguous mangrove forest and a designated
26 UNESCO World Heritage Site, is situated in the tidally active lower deltaic plain of
27 the Ganges-Brahmaputra-Meghna basin along the Bay of Bengal (UNESCO, 2025).
28 Spread approximately 10,000 km² across India and Bangladesh, this unique ecosys-
29 tem supports the livelihoods of around 7.2 million people (Nishat et al., 2019). It
30 provides critical ecosystem services, including acting as a natural buffer against
31 cyclones, coastal erosion, and other environmental hazards (Mukul et al., 2019).
32 The Sundarbans play a key role both ecologically, by protecting the area from
33 coastal erosion, and for people's livelihoods, by providing resources such as honey,
34 fuelwood, and fish (Kibria et al., 2018).

35 In the Sundarbans region, agricultural land is being abandoned in favour of
36 shrimp aquaculture, and due to increasing salinity level and freshwater scarcity, the
37 region is experiencing a rise in water-borne diseases (Dasgupta et al., 2020). A
38 World Bank study has projected large-scale climate-induced migration from the
39 fringes of the Sundarbans (Nishat et al., 2019).

40 This world's largest mangrove forest is composed of a network of low-lying
41 conglomeration islands created from sediment loads deposited from the Himalayan
42 rivers (Ghosh et al., 2015). These islands are of mudflats with salt pans and natural
43 levees that are separated by tidal creeks (Siddiqi, 2001) and provide the world's
44 largest remaining habitat for the globally endangered Bengal tiger (*Panthera tigris*
45 *tigris*) (Mukul et al., 2019). This ecosystem, located in a tropical cyclone belt, dem-
46 onstrates a complex interaction between social and ecological systems (Kibria et al.,
47 2018). The fluctuating water levels, temperature, and wind flow are affecting the
48 topography of the area, making it prone to several natural hazards, leading to the
49 destruction of forest resources (Jandl et al., 2007). Studies have recommended an
50 integrated approach that envisages the ecological and adjacent socio-cultural sys-
51 tems to be reconciled for natural hazards protection, livelihood improvement, and
52 poverty alleviation (Sayer et al., 2013). The Indian vision emphasises community
53 wellbeing, ecosystem conservation and phased out-migration. The Bangladesh
54 vision emphasises the management and conservation of the delta (IUCN, 2014).
55 Studies have indicated that the majority of the forested grids in the region are likely
56 to experience a shift in forest types due to climate change scenarios (Ravindranath
57 et al., 2006). A study on the comparison of the area with earlier survey records (e.g.
58 early nineteenth-century Dampier and Hodges survey of forest extent) indicates that

the mangrove has shrunk to almost half in size (DasGupta & Shaw, 2017). Previous studies have indicated that the anthropogenic interference began in the region in the late eighteenth century, mainly through agricultural practices (Ghosh et al., 2015), and deforestation is contributing 6–17% of anthropogenic CO₂ emission (2000–2010, about 1.0 Pg C/year was emitted) (Baccini et al., 2012).

As mentioned above, the Sundarbans is increasingly threatened by a combination of anthropogenic pressures and natural forces (Sievers et al., 2020). The degradation of forest cover and associated resources is driven by deforestation, land-use change, and the rising frequency of climate-induced events such as cyclones, floods, and droughts (Karsch et al., 2023). Many villages have already witnessed the disappearance of protective mangrove belts, which serve as the region's first line of defence against climate change impacts. The intrusion of seawater has led to increased salinity, resulting in the decline of high-value, storm-resistant tree species such as Sundari (*Heritiera fomes*), from which the Sundarbans derives its name. This ecological stress is further exacerbated by reduced freshwater and sediment inflows due to upstream damming and river regulation (Dasgupta et al., 2020). The consequences are visible and alarming: several mangrove islands have vanished over the past century, others have significantly shrunk in the last 50 years, and repeated embankment failures have displaced communities and destroyed homes.

In this chapter, we discuss key data sources that can be utilised for long-term assessment of the ecological and socioeconomic conditions of the Sundarbans.

1.1 Study Area

This study investigates the current extent of the Sundarbans mangrove ecosystem and its adjacent regions that used to be mangrove forests (Fig. 1). We demonstrate the utility of archived historic geospatial data sets to highlight regions where there is a loss of land or of mangroves over the last 175 years.

1.2 Analytical Framework

The study followed a four step workflow: (1) georeferencing of archived topographic maps (root mean square error (RMSE) < 50 m) using identifiable ground control points, (2) mosaicking and orthorectification of CORONA KH-4B film scans, (3) overlay and change detection with modern satellite imagery in ArcGIS Pro and QGIS, and (4) quantitative estimation of mangrove loss and land conversion using supervised classification and manual visual interpretation. This framework ensured comparability across disparate data sets collected over a span of nearly 250 years.



Fig. 1 The study area showing the current extent of mangroves in India and Bangladesh

94 **1.3 Remote Sensing Data**

95 A wide range of satellite imagery is now available for mapping the current extent of
 96 the Sundarbans mangrove ecosystem, with near-daily acquisitions from multiple
 97 platforms. In this study, we utilise imagery from Landsat and PlanetScope satellites.
 98 The Landsat programme has been providing global-scale remote sensing data since
 99 1972, while PlanetScope has offered near-daily coverage in recent years (Planet
 100 Team, 2019). These data sets are widely used for various Earth resource analyses,
 101 including vegetation mapping and monitoring in the Sundarbans. Given the avail-
 102 ability of well-established algorithms for vegetation classification and condition
 103 assessment using these missions, this chapter focuses on the use of historic, high-
 104 resolution, declassified satellite imagery from the CORONA mission to comple-
 105 ment contemporary analyses.

106 The USA's Corona mission, which was the first satellite-based remote sensing
 107 mission operational during 1960–1972 (CIA, 2025). These satellites, code-named
 108 as CORONA, ARGON, and LANYARD, collected more than 860,000 images of
 109 the Earth's surface covering 1900 million square kilometres. The USA's National
 110 Archives and Records Administration (NARA) was given the responsibility for the
 111 original film and provided access to a duplicate copy for public viewing of the film.
 112 The USGS was also provided a copy to support science products. The data set can
 113 be accessed from the USGS's Earth Explorer website (USGS, 2025a, 2025b).

A number of camera systems were used for collecting photographic films. The earlier missions carried a single panoramic camera (KH-1, KH-2, KH-3, and KH-6) or a single frame camera (KH-5). The later systems carried two panoramic cameras with a separation angle of 30°, with one camera looking forward and the other looking aft (KH-4, KH-4A, and KH-4B) (USGS, 2025a, 2025b).

For this study, we used images acquired in 1972 by the CORONA satellite with the KH-4B camera that had a spatial resolution of 1.8 m. The images were grey-scale single band, and the interpretation was based on the tone, texture, patterns, shadow, shape, and size of various features. The images were scanned using high-performance photogrammetric film scanner to create digital products at 7 micron or 14 micron resolutions, and the scanned images can be subjected to photogrammetry for 3d information extraction (USGS, 2025a, 2025b).

The images are available in different parts for each panoramic scene, and for merging all the image parts, a specialised stereogrammetry software was used. The open-source software from NASA, AMES Stereo Pipeline (ASP), was used to stitch the individual film scans to generate a whole image (Beyer et al., 2018) (Fig. 2).

The images collected from two different angles were downloaded (DA and DF series), and a mosaic was created for the study area using ArcGIS Pro software (Figs. 3 and 4). The KH4A had a dual panoramic camera system with fore (forward) and aft (backward) looking cameras having a 15° off-nadir view angle, resulting in a convergence angle of 30° and a baseline-to-height ratio of 0.54. The images were named as DF and DA series for and alt looking cameras (Figs. 3 and 4).

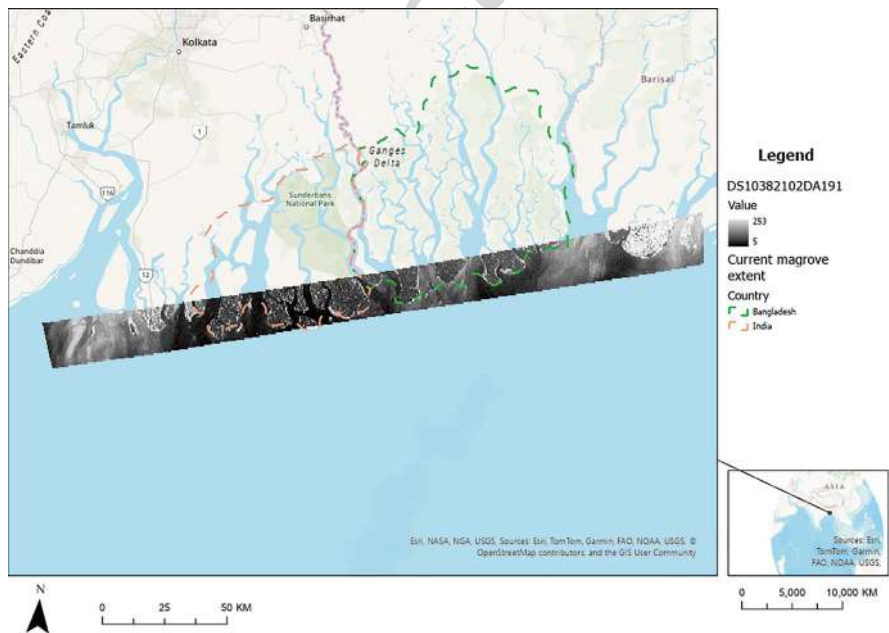


Fig. 2 An example stitched panoramic scene taken from the CORONA satellite

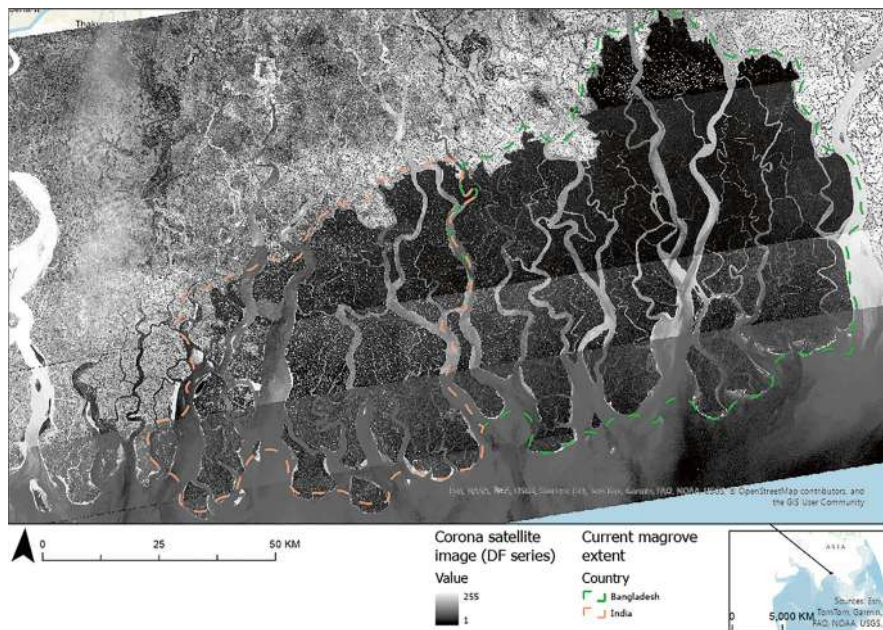


Fig. 3 The mosaic was created for the study area using images collected in the DF series. The DF series had the forward coverage with the camera set in panoramic forward mode

136 The mangrove areas were represented by a darker tone in the image and were
 137 identified by their distinct shapes. The detailed version of the map shows loss of
 138 land masses with mangroves in the southwestern part of the Sundarbans in the last
 139 50 years (Fig. 5). The CORONA image is compared with the current mangrove
 140 boundaries derived from the mosaic of PlanetScope images (Srivastava et al., 2025).
 141 The selection of PlanetScope imagery was motivated by its near-daily revisit fre-
 142 quency and 3–5 m spatial resolution (Planet, 2025), which enables the detection of
 143 fine-scale land-use changes that coarser platforms such as MODIS or even Sentinel-2
 144 may miss. For vegetation condition assessment, standard indices such as NDVI and
 145 EVI were derived, and in saline-dominated tracts, radar vegetation indices (RVI)
 146 from Sentinel-1 SAR were also considered to improve classification robustness in
 147 persistently cloudy conditions.

148 A detailed comparison at a finer map scale in the northern part of the Sundarbans
 149 reveals progressive encroachment of mangrove forests by agricultural activities.
 150 This transformation began around 1780 and continued until 1875, when large areas
 151 of mangroves were cleared for cultivation (Mahmood et al., 2021). Subsequently,
 152 between 1876 and 1951, further deforestation occurred to support timber produc-
 153 tion and generate revenue. From 1952 onward, several conservation and manage-
 154 ment plans were introduced to protect the region (Mahmood et al., 2021). However,
 155 satellite imagery from 1972 to 2020 reveals continued agricultural expansion into
 156 mangrove areas, underscoring the ongoing pressures on this fragile ecosystem
 157 (Fig. 6).

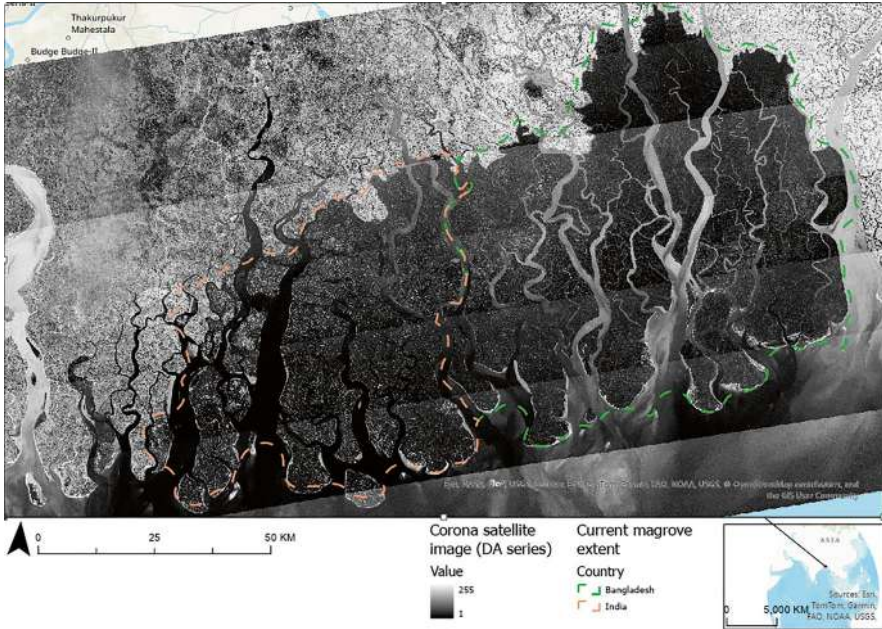


Fig. 4 The mosaic was created for the study area using images collected in the DA series. The DA series collected images in aft (backward) panoramic mode

1.4 Topographic Maps

158

Topographic maps offer a comprehensive overview of the landscape by depicting key natural and human-made features with precision. Their accuracy stems from data collected through systematic ground surveys conducted by trained professionals, followed by meticulous cartographic plotting. As part of national mapping programmes, these maps adhere to standardised specifications for representing surface features, which are consistently tied to the scale of the map series.

159
160
161
162
163
164

The Survey of India, established in 1767, laid the foundation for mapping the Indian subcontinent. However, systematic mapping of Earth’s surface features began only in the latter half of the nineteenth century (Coldstream, 1919). Early maps were produced at coarse scales, limiting their detail and utility. In the early twentieth century, a structured topographic survey scheme was introduced, beginning with maps at a 1:1 million scale (covering 4° latitude × 4° longitude). These were subsequently subdivided into 16 sheets at a 1:250,000 scale, each covering 1° latitude × 1° longitude (Edney, 1991).

165
166
167
168
169
170
171
172

For this study, the earliest map utilised was from the 1:250,000 scale series, published in 1913, based on survey data collected between 1895 and 1900, with some hydrological information dating back to 1878 (Fig. 5). Additional maps used in this analysis were drawn from the 1:50,000 to 1:63,000 series (Brown, 2023), most of which were published in the 1920s and 1940s. The 1920s maps incorporated data

173
174
175
176
177

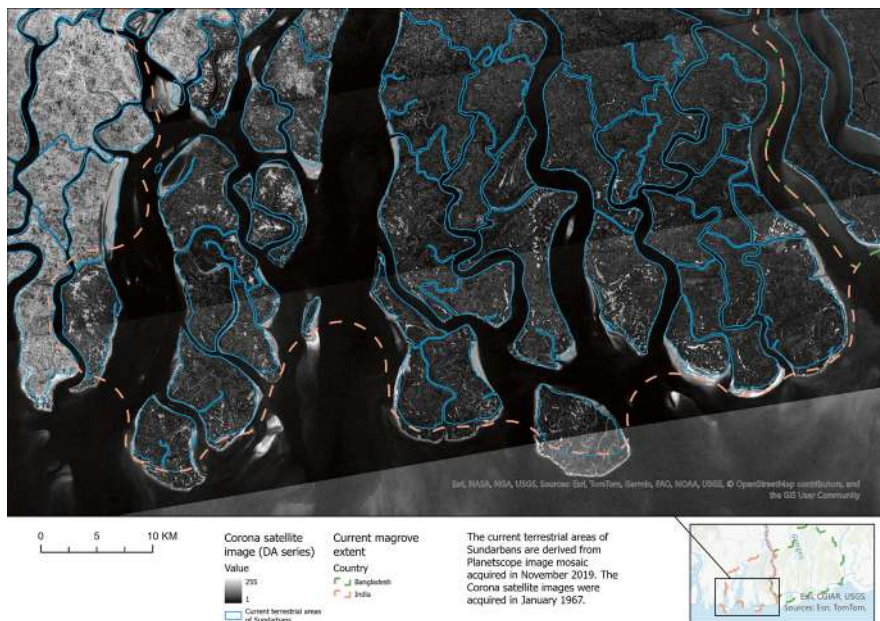


Fig. 5 The southern part of the Sundarbans shows a loss of land over the past 50 years. The blue polygons represent the current extent of Sundarbans mangroves, which are derived from PlanetScope data

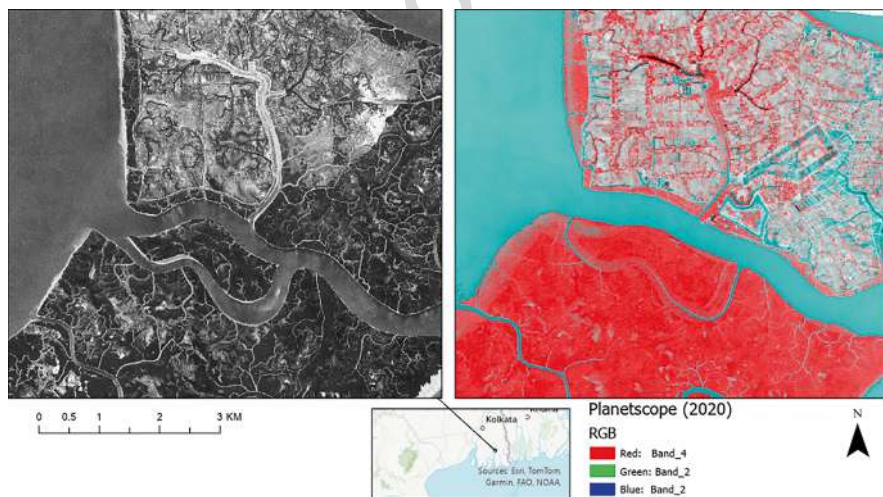


Fig. 6 A local scale comparison between CORONA (1972) and PlanetScope (2020) images showing the conversion of mangrove forests to agricultural lands

collected primarily between 1904 and 1908, while the 1940s maps combined earlier survey data with new information gathered in the 1920s and updates derived from aerial photography conducted in the 1940s. Collectively, these maps offer a valuable historical perspective of the region's landscape (Fig. 6).

The largest-scale maps available for the region were produced at approximately 1:50,000 scale and were published primarily during the 1920s and 1940s (Fig. 7). For this study, the earliest map utilised was from the 1:250,000 scale series, published in 1913, based on survey data collected between 1895 and 1900, with some hydrological information dating back to 1878. Additional maps used in this analysis were drawn from the 1:50,000 to 1:63,000 series (Brown, 2023), most of which were published in the 1920s and 1940s. The 1920s maps incorporated data collected primarily between 1904 and 1908, while the 1940s maps combined earlier survey data with new information gathered in the 1920s and updates derived from aerial photography conducted in the 1940s. Collectively, these maps offer a valuable historical perspective of the region's landscape (Fig. 8).

Several historic topographic maps are available at coarse resolutions. Notably, the region was surveyed by British surveyors in the early eighteenth century, culminating in the publication of a complete map of the study area in 1761, based on survey data collected in 1760 (Fig. 9). Many of these early maps are poorly drawn and lack precise geographic coordinates, making georeferencing a significant challenge. Their limited spatial accuracy and incomplete metadata further complicate integration with modern geospatial data sets.

Another significant topographic map, available from the mid-nineteenth century, was produced at an approximate scale of 1:250,000. This map includes latitude and longitude coordinates, enabling accurate georeferencing using GIS software. Published in 1853, it was based on survey data collected between 1847 and 1851 (Fig. 10) and primarily covers the western portion of the Sundarbans. A comparative analysis with recent Landsat 8/9 imagery reveals notable mangrove forest loss, particularly in the northern and western regions of the study area (Fig. 10).

The western part of the Sundarbans has undergone significant transformation, with large areas converted into human settlements, including villages, small towns, agricultural lands, and road networks (Fig. 11). These regions now show no visible signs of mangrove forests. Mangrove ecosystems are well-known for their role in mitigating the adverse impacts of cyclones and sea-level rise. However, the western Sundarbans is now highly susceptible to coastal erosion (Mohammed et al., 2024). The replacement of mangroves with agricultural and residential land use increases the vulnerability of these areas to extreme weather events and long-term environmental degradation.

The northern part of the region, once dominated by mangrove forests, has also experienced significant encroachment by human settlements and is now largely characterised by aquaculture activities. In the Landsat false-colour composite imagery, dark blue patches clearly indicate the presence of aquaculture ponds and facilities (Fig. 12). This transformation reflects a shift in land use that has implications for ecosystem health and resilience. The destructive aquaculture practices of the past are well-known to destroy mangrove forests in the region (Parvin et al., 2023).

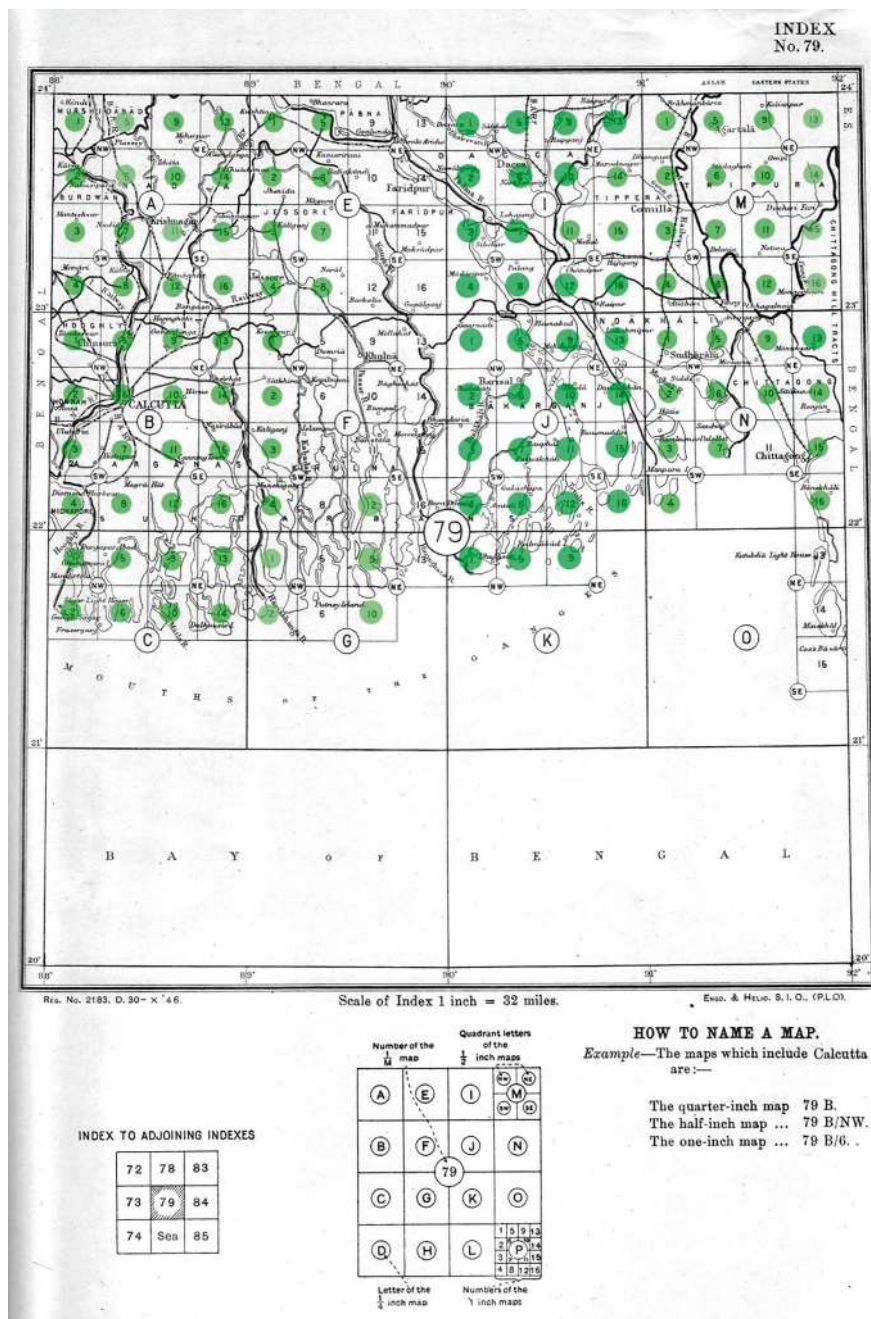


Fig. 7 The coverage of India and the surrounding regions by topographic maps (1:50–63,000) in the Sundarbans region (source: Brown, 2023)



Fig. 8 The current extent of the mangrove vegetation is distributed across India and Bangladesh. The earlier extent was much larger, which can be seen in topographic maps published in the early twentieth century. These toposheets are available at roughly 1:63,000 map scale and were published in the early and mid-twentieth century. The recent topographic maps can be obtained from the survey departments of India and Bangladesh

A well-established human settlement in the region can be seen in the photographs taken by the authors during a field visit to the area, featuring aquaculture ponds, road networks, residential structures, agricultural fields, and railway tracks (Fig. 13). While exploring Google Street View, we noticed several other anthropogenic structures such as railway tracks and mobile towers.

1.5 *Combining Historic Topographic Maps with Declassified Images and Recently Acquired Remote Sensing Data*

Integrating multiple archival data sets offers valuable insights into the long-term ecological dynamics of ecosystems. Such an approach is particularly critical for future management, as climate projections indicate an increased frequency of extreme weather events, which could severely impact ecosystem health and, consequently, local livelihoods (Sarkar et al., 2024). This strategy becomes even more important in regions like the Sundarbans, where large areas are inaccessible and inhabited by wildlife, making remote sensing-based desktop analyses the most practical and effective method for monitoring and assessment (Srivastava et al., 2025).

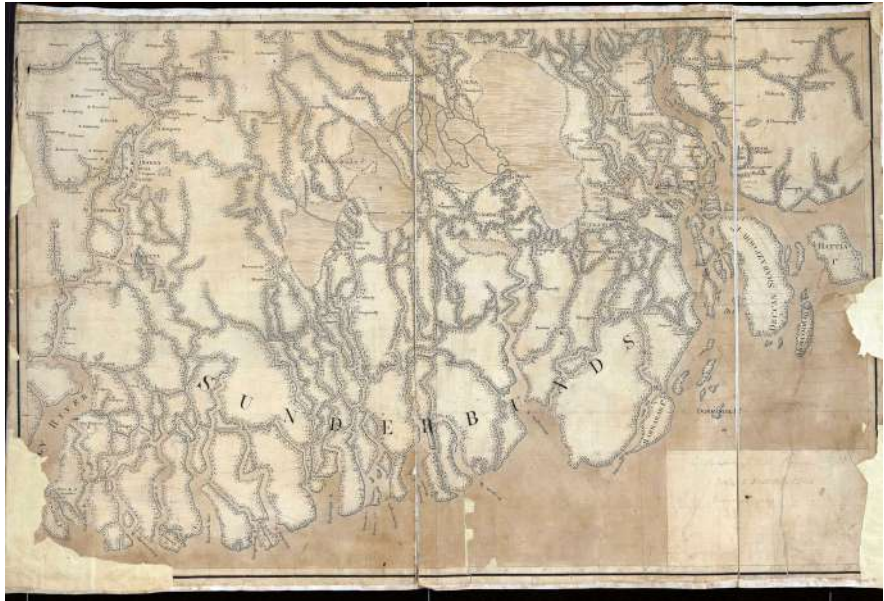


Fig. 9 The oldest topographic map of Sundarbans available at the scale of approximately 1:300,000. The map was published in 1761, and the area was surveyed in 1760. This map has geographic area and map scale, but key coordinate information is missing, making georeferencing a challenge (source: Brown, 2023)

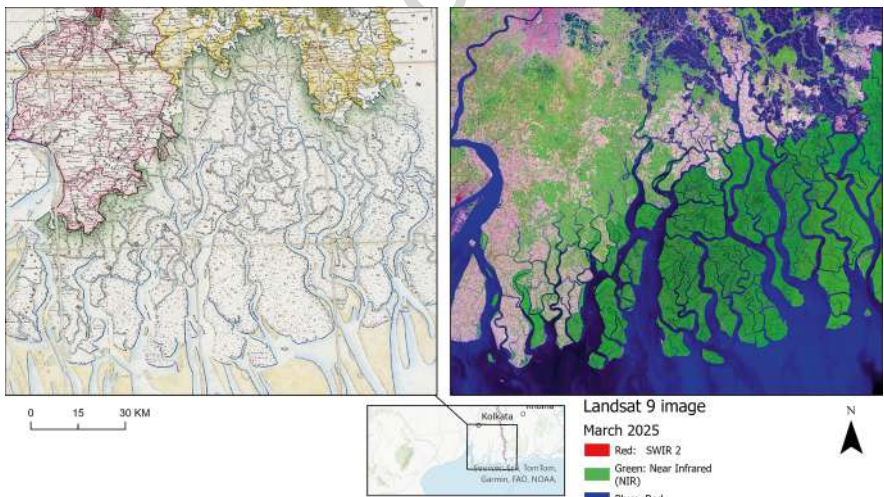


Fig. 10 The topographic map, prepared in 1853 from survey data collected between 1847 to 1851 clearly shows a much larger northern extent of the Sundarbans mangroves when compared with a recently acquired Landsat 9 image. The dark green colour in the Landsat image indicates mangrove forests. These mangrove forests are replaced by urban areas and agricultural fields on the western and northern sides

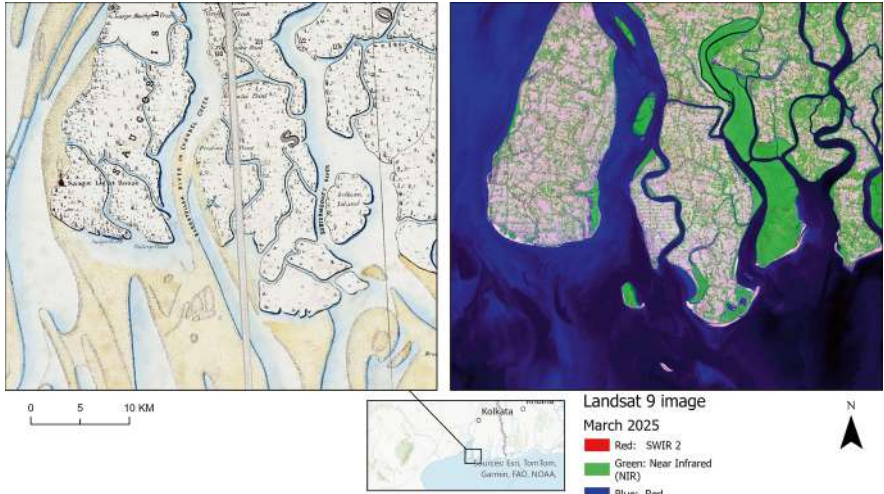


Fig. 11 The detailed version of Fig. 8 focuses on the western part of the Sundarbans, which is now fully converted to small towns, villages, and agricultural fields with road networks

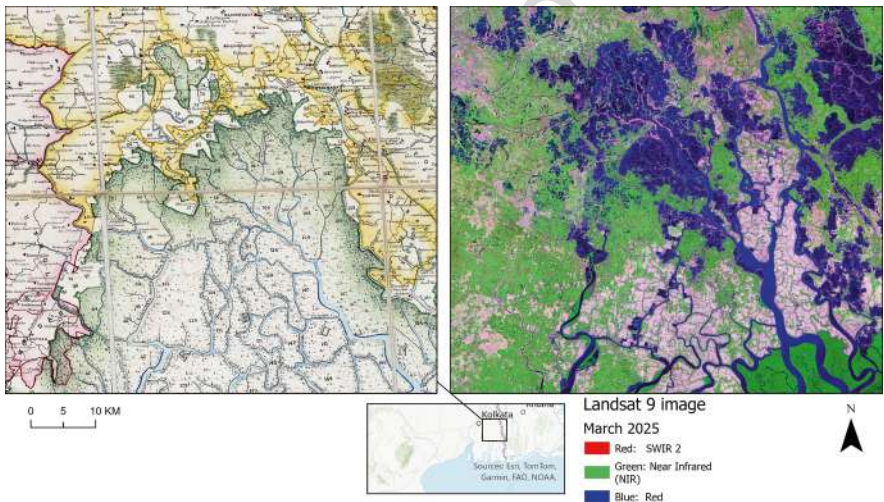


Fig. 12 The detailed version of Fig. 8 focuses on the northern part of the Sundarbans, which is now fully converted to small towns, villages and agricultural fields with road networks

The topographic maps published in 1922, based on survey data collected in 1905 239
primarily for revenue purposes, provide valuable insights into the ecological conditions of that period (Fig. 14). When compared with the 1942 topographic map, clear 240
evidence of anthropogenic encroachment and land loss emerges. Further comparison 241
with remote sensing imagery from the early 1970s reveals continued changes in 242
both landmass and mangrove cover. A recent Landsat image highlights significant 243
244



Fig. 13 Photographs taken in the northern part of the regions mentioned in Fig. 10. This area was a mangrove forest in the past, but now it is an established human settlement with aquaculture ponds, houses, power lines, and roads (source: photographs taken by authors, February 2023)

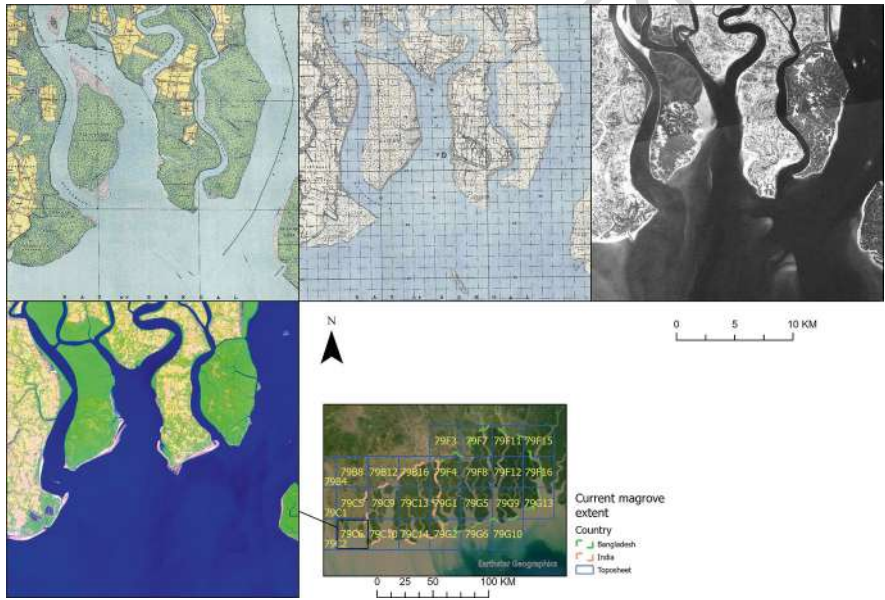


Fig. 14 A comparison of geospatial information collected over 120 years. The information is from early and mid-twentieth-century topographic maps, CORONA satellite data collected in the 1970s, and a recent Landsat 9 image. An anthropogenic conversion of a mangrove ecosystem into human settlement can be seen in one of the islands that were dominated by mangroves in the year 1905

245 transformations, particularly in the southern part of the region, underscoring the
 246 extent of ecological change over time (Fig. 15).

247 Recent Google Earth Street View imagery of the same area reveals that land once
 248 covered by mangrove forests has been transformed into a well-established human

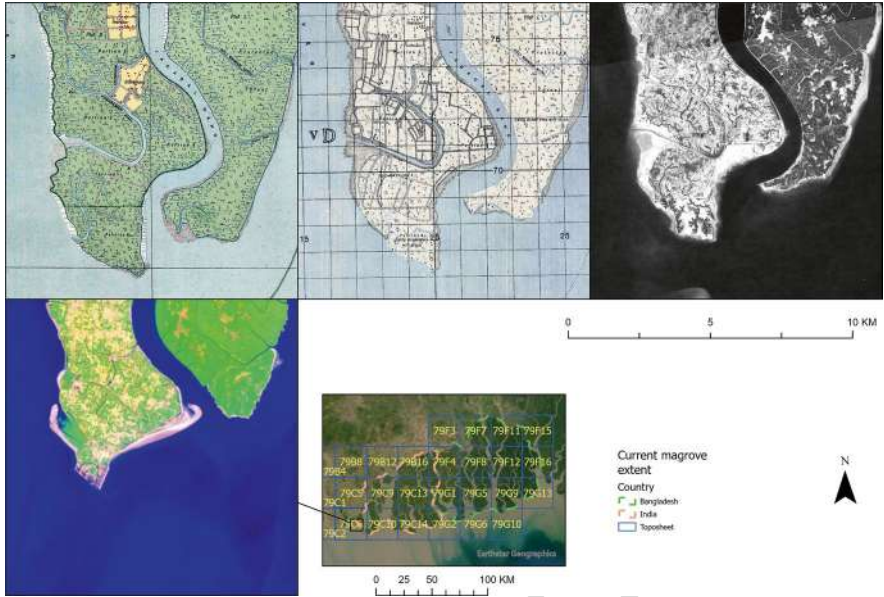


Fig. 15 A detailed view of the southern end of the island, where mangrove forests are totally lost. Land loss over time can also be noticed in the southern end, mostly in the last 50 years



Fig. 16 Examples of mangrove area converted into human settlements showing commuters, power lines, roads, and houses (source: photographs taken by authors, February 2023)

settlement. The area now features a connected network of roads, residential buildings, agricultural fields, communication towers, power lines, and people commuting for work (Fig. 16). The recent conversions of agricultural fields to aquaculture farms have been a concern for this ecosystem (Sumon et al., 2025).

249
250
251
252

253 2 Conclusions and Recommendations

254 Archived data sets play a vital role in long-term ecological monitoring, offering
255 critical insights that inform future planning and conservation strategies for sensitive
256 ecosystems. Many human settlements are increasingly vulnerable to extreme
257 weather events, particularly in areas where natural ecosystems—once capable of
258 buffering such impacts—have been degraded or lost. With advancements in data
259 processing and image analysis technologies, it is now possible to extract meaningful
260 information from historical landscape records. This enables the identification of
261 high-risk regions and supports more targeted efforts to preserve and restore ecologi-
262 cally significant areas.

263 A variety of additional sources can be utilised to enrich long-term ecological
264 assessments, including archived aerial photographs of the region. Beyond topo-
265 graphic maps and satellite imagery, nonspatial historical records containing geo-
266 graphic descriptions also offer valuable context for understanding ecosystem
267 changes over time. Integrating these diverse data sources using modern geospatial
268 technologies and recent high-resolution data sets enables a more comprehensive
269 reconstruction of past landscapes and supports more informed conservation and
270 management strategies.

271 Future research should increasingly integrate high-resolution LiDAR and UAV
272 photogrammetry for canopy structure mapping, SAR time-series (Sentinel-1, ALOS
273 PALSAR) for salinity and inundation monitoring, and machine learning-based
274 change detection algorithms for automated analysis of multi-temporal data sets.
275 Such innovations, when combined with archived historical baselines, can provide a
276 holistic monitoring system that not only tracks ecological integrity but also antici-
277 pates areas most vulnerable to sea-level rise and human encroachment.

278 **Acknowledgement** The book chapter is written from the study under the Multinational
279 Collaborative Project partially supported by Asia Pacific Network for Global Change Research
280 (APN-GCR) and University of the Sunshine Coast (UniSC), Australia. The logistic support from
281 Indian Council of Agricultural Research, Department of Agricultural Research and Education,
282 Govt. of India for the study is duly acknowledged.

283 References

- 284 Baccini, A., Goetz, S., Walker, W., Laporte, N., Sun, M., Sulla-Menashe, D., Hackler, J., Beck, P.,
285 Dubayah, R., & Friedl, M. (2012). Estimated carbon dioxide emissions from tropical deforestation
286 improved by carbon-density maps. *Nature Climate Change*, 2(3), 182–185.
- 287 Beyer, R. A., Alexandrov, O., & McMichael, S. (2018). The Ames Stereo Pipeline: NASA's open
288 source software for deriving and processing terrain data. *Earth and Space Science*, 5(9),
289 537–548.
- 290 Brown, J. (2023). *79 Block—63k or 50k scale Maps of South Asia*. Zenodo 2023. [https://doi.
291 org/10.5281/zenodo.7869274](https://doi.org/10.5281/zenodo.7869274)

- CIA. (2025). *CORONA: America's First Imaging Satellite Program 2025* [cited August 2025]. <https://www.cia.gov/legacy/museum/exhibit/corona-americas-first-imaging-satellite-program/> 292
293
- Coldstream, W. M. (1919). *Survey of India maps. Vol. 7, Records of the Survey of India*. Photo Litho Office. 294
295
- DasGupta, R., & Shaw, R. (2017). Perceptive insight into incentive design and sustainability of participatory mangrove management: a case study from the Indian Sundarbans. *Journal of Forestry Research*, 28(4), 815–829. 296
297
298
- Dasgupta, S., Wheeler, D., Sobhan, M. I., Bandyopadhyay, S., & Paul, T. (2020). Coping with climate change in the Sundarbans: Lessons from multidisciplinary studies. World Bank Publications. 299
300
301
- Edney, M. H. (1991). The atlas of India 1823–1947/the natural history of A topographic map series. *Cartographica*, 28(4), 59–91. 302
303
- Ghosh, A., Schmidt, S., Fickert, T., & Nüsser, M. (2015). The Indian Sundarban mangrove forests: History, utilization, conservation strategies and local perception. *Diversity*, 7(2), 149–169. 304
305
- IUCN. (2014). *Bangladesh Sundarban Delta Vision 2050: A first step in its formulation*. International Union for Conservation of Nature. 306
307
- Jandl, R., Lindner, M., Vesterdal, L., Bauwens, B., Baritz, R., Hagedorn, F., Johnson, D. W., Minkinen, K., & Byrne, K. A. (2007). How strongly can forest management influence soil carbon sequestration? *Geoderma*, 137(3–4), 253–268. 308
309
310
- Karsch, G., Mukul, S. A., & Srivastava, S. K. (2023). Annual mangrove vegetation cover changes (2014–2020) in Indian Sundarbans National Park using Landsat 8 and Google Earth Engine. *Sustainability*, 15(6), 5592. 311
312
313
- Kibria, A., Costanza, R., Groves, C., & Behie, A. M. (2018). The interactions between livelihood capitals and access of local communities to the forest provisioning services of the Sundarbans Mangrove Forest, Bangladesh. *Ecosystem Services*, 32, 41–49. 314
315
316
- Mahmood, H., Ahmed, M., Islam, T., Uddin, M. Z., Ahmed, Z. U., & Saha, C. (2021). Paradigm shift in the management of the Sundarbans mangrove forest of Bangladesh: Issues and challenges. *Trees, Forests and People*, 5, 100094. 317
318
319
- Mohammed, Sultana, F., Khan, A., Ahammed, S., Saimun, M. S. R., Bhuiyan, M. S., Srivastava, S. K., Mukul, S. A., & Arfin-Khan, M. A. (2024). Assessing vulnerability to cyclone hazards in the world's largest mangrove forest, The Sundarbans: A geospatial analysis. *Forests*, 15(10), 1722. 320
321
322
323
- Mukul, S. A., Alamgir, M., Soheli, M. S. I., Pert, P. L., Herbohn, J., Turton, S. M., Khan, M. S. I., Munim, S. A., Reza, A., & Laurance, W. F. (2019). Combined effects of climate change and sea-level rise project dramatic habitat loss of the globally endangered Bengal tiger in the Bangladesh Sundarbans. *Science of the Total Environment*, 663, 830–840. 324
325
326
327
- Nishat, B., Rahman, A., & Mahmud, S. (2019). *Landscape narrative of the Sundarban: Towards collaborative management by Bangladesh and India*. World Bank Group. 328
329
- Parvin, S., Sakib, M. H., Islam, M. L., Brown, C. L., Islam, M. S., & Mahmud, Y. (2023). Coastal aquaculture in Bangladesh: Sundarbans's role against climate change. *Marine Pollution Bulletin*, 194, 115431. 330
331
332
- Planet. (2025). *Planet Explorer 2025* [cited January 2025]. <https://www.planet.com/explorer/> 333
- Planet Team. (2019). *Planet application program interface: In space for life on Earth 2025* [cited December 2019]. <https://api.planet.com/> 334
335
- Ravindranath, N. H., Joshi, N. V., Sukumar, R., & Saxena, A. (2006). Impact of climate change on forests in India. *Current Science*, 90(3), 354–361. 336
337
- Sarkar, P., Banerjee, S., Biswas, S., Saha, S., Pal, D., Naskar, M. K., Srivastava, S. K., Barman, D., Kar, G., & Mukul, S. A. (2024). Contribution of mangrove ecosystem services to local livelihoods in the Indian Sundarbans. *Sustainability*, 16(16), 6804. 338
339
340
- Sayer, J., Sunderland, T., Ghazoul, J., Pfund, J.-L., Sheil, D., Meijaard, E., Venter, M., Boedihartono, A. K., Day, M., & Garcia, C. (2013). Ten principles for a landscape approach to reconciling agriculture, conservation, and other competing land uses. *Proceedings of the National Academy of Sciences*, 110(21), 8349–8356. 341
342
343
344

- 345 Siddiqi, N. (2001). Mangroves of Bangladesh Sundarbans and accretion areas. In *Mangrove eco-*
346 *systems functions management*. Springer-Verlag.
- 347 Sievers, M., Chowdhury, M. R., Adame, M. F., Bhadury, P., Bhargava, R., Buelow, C., ... &
348 Connolly, R. M. (2020). Indian Sundarbans mangrove forest considered endangered under Red
349 List of Ecosystems, but there is cause for optimism. *Biological conservation*, 251, 108751.
- 350 Srivastava, S. K., Mukul, S., Banerjee, S., Barman, D., Kar, G., Hindersah, R., Arief, M. C. W., &
351 Khan, M. A. S. A. (2025). A hierarchical and inclusive zonation of Sundarbans for monitoring
352 and management of the world heritage area. *APN Science Bulletin*, 15(1), 1–18.
- 353 Sumon, K. A., Kanok, N. J. R., Sadat, M. A., Mainuddin, M., Wahid, S. M., & Karim, F. (2025).
354 A comprehensive review on the negative impacts on Sundarbans fisheries: Insights from the
355 hydrological changes modulated by climate change and anthropogenic activities. *Marine*
356 *Pollution Bulletin*, 220, 118409.
- 357 UNESCO. (2025). *The Sundarbans*. UNESCO World Heritage Convention 2025 [cited August
358 2025]. <https://whc.unesco.org/en/list/798/>
- 359 USGS. (2025a). *USGS Earth Explorer 2025* [cited January 2025]. <https://earthexplorer.usgs.gov/>
- 360 USGS. (2025b). *USGS EROS archive—Declassified data—Declassified satellite imag-*
361 *ery—1* 2025 [cited August 2025]. [https://www.usgs.gov/centers/eros/science/](https://www.usgs.gov/centers/eros/science/usgs-eros-archive-declassified-data-declassified-satellite-imagery-1)
362 [usgs-eros-archive-declassified-data-declassified-satellite-imagery-1](https://www.usgs.gov/centers/eros/science/usgs-eros-archive-declassified-data-declassified-satellite-imagery-1)